Retention behavior of metal particle dispersions in aqueous and nonaqueous carriers in thermal field-flow fractionation

Paul M. Shiundu[a],*, Stephen M. Munguti[a], S. Kim Ratanathanawongs Williams[b]

[a]*Department of Chemistry, University of Nairobi, P.O. Box 30197, Nairobi, Kenya*
[b]*Colorado School of Mines, Department of Chemistry and Geochemistry, Golden, CO 80401, USA*

Abstract

Until quite recently, theories on thermophoresis of particles predicted very low thermophoretic velocities of metal particles in liquids. This prediction was based on the understanding that the very high thermal conductivities of metals relative to most liquid media resulted in quite low temperature gradients across the metal particle thereby leading to low net force on the particle. In this paper, we report the retention behavior of submicrometer size metal particles of silver (Ag), gold (Au), palladium (Pd) and platinum (Pt) suspended in both aqueous and organic (specifically, acetonitrile and tetrahydrofuran) carrier liquids in thermal field-flow fractionation (ThFFF). The dependence of the metal particle retention on various factors such as particle composition, amount of added electrolyte, carrier liquid composition, field strength, channel thickness, and carrier flow-rate is evaluated and discussed. A comparison in particle retention behavior among equal-sized metal, latex and silica particles is also provided.
© 2002 Elsevier Science B.V. All rights reserved.

Keywords: Field-flow fractionation; Thermal field-flow fractionation; Thermophoresis; Metal particles

1. Introduction

Thermal field-flow fractionation (ThFFF) is an analytical-scale technique whose operation is controlled in part by thermal diffusion coefficient, D_T, a basic transport coefficient describing the movement of matter under an applied temperature gradient. Over the recent past, this technique that relies on thermophoresis to separate and characterize polymeric and colloidal materials, has proven to be useful for the determination of thermal diffusion coefficient data or thermophoretic mobilities of latex

and silica particles suspended in aqueous and/or nonaqueous carrier suspensions [1–4]. The ready compatibility of ThFFF apparatus with both aqueous and nonaqueous carrier solutions affords the technique great flexibility for investigating the phenomenon of thermophoresis of particles in various liquid suspensions. It is therefore not surprising that in this study, ThFFF is the technique of choice for the investigation of thermophoresis of metal particles suspended in both aqueous and nonaqueous carrier media.

According to the theory of phoretic motion of solid particles in a liquid, the magnitude of the temperature gradient across a particle determines the thermophoretic velocity of the particle [5]. The

---

implication of the theory therefore is that for materials of high thermal conductivities such as metal particles, quite low thermophoretic velocities are predicted due to low temperature gradients expected across the particle. Earlier theoretical [6–8] and experimental [9] investigations of thermophoresis in a liquid predict low thermophoretic velocities of metal particles in comparison with nonmetal particles. Our present experimental data on the retention behavior of submicrometer metal particles in a ThFFF apparatus however, suggest otherwise. This has prompted us to examine other models in existence that might shed some light in this challenging area of thermophoresis.

In a theoretical article by Giddings et al. [10], the role of surface potential distribution and thermophoretic velocities of metal particles was examined. In the article, the attractive electrostatic potential of a double layer and a surface potential with a secondary minimum were considered as important parameters in the thermophoretic motion of metal particles. The model also predicted comparable thermophoretic velocities of equal-sized metal and ''normal'' particles and suggested that differences in their velocities could vary depending mainly on the shape of the potential energy curve. The basis for this prediction was that, despite the practically zero surface temperature gradient of about $10^{-3} \nabla T$, considerations of ''spatial'' temperature distribution over a thin surface layer of the particle (about a tenth of the particle radius) yields temperature gradients as high as $0.15\nabla T$. Hence the expectation that quite large thermophoretical velocities for metal particles is possible. The model could also be used to explain the thermophoretic behavior of other solid particles (such as silica) suspended in electrolyte-containing liquids. In these, ion adsorption would result in the establishment of a double layer at the particle surface, from where the ''spatial'' temperature distribution would be achieved. This model however, cannot be considered to be exhaustive because it does not explain all the features of various particle retention behavior observed in ThFFF. Specifically, the model fails to account for previous experimental observations that (i) latex or (and) silica particle thermophoretic mobilities and therefore their retention in ThFFF depend on particle size; (ii) latex or (and) silica particle thermophoretic mobilities may

increase or decrease with salt concentration in a given carrier liquid [1–4,11–13] and (iii) the carboxylated PS latex particles have the same thermophoretic properties as unmodified particles in acetonitrile when tetrabutylammonium perchlorate is the only additive [3].

The model developed by Schimpf and Semenov [14] for polymer thermophoresis takes a similar approach to the model described above for suspended particles [10]. The former has been used in part, to give a qualitative interpretation of the experimentally reported differences in thermophoretic properties between polymeric particles and their polymer counterparts of similar chemical composition [13]. For instance, whereas the thermophoresis of suspended acrylonitrile–butadiene–styrene (ABS) particles is dependent on salt concentration, thermophoresis of ABS polymer is independent of salt concentration. In this model, it was proposed that the slip flow of a liquid around the surface of a dilute component dissolved in the liquid is induced by an osmotic pressure gradient. The source of this gradient is different for suspended particles and dissolved polymers. For particles, the osmotic pressure gradient is produced by a gradient in the concentration of dissolved solutes near the particle surface. In the absence of a salt, the particle–solvent interaction constant in some solvents is too small to produce a concentration and thus a pressure gradient. Hence the near lack of thermophoretic mobility of particles in some salt-free suspending media. In contrast, the osmotic pressure gradient in polymer solutions is produced solely by a gradient in the concentration of solvent molecules, with a resultant strong enough slip flow to induce thermophoresis of the monomer units of the polymer in organic solvents where the monomer unit–solvent interaction forces are large.

As a follow-up to the model discussed in the preceding paragraph, Semenov [15,16] has proposed two theoretical models in an attempt to account for the previously unexplained features of particle retention in a ThFFF system. The first model highlights the possible role of concentration polarization phenomena to explain thermophoresis of particles in a liquid [15]. In the second model [16], thermophoresis of particles in a liquid electrolyte is examined theoretically and it is shown that a suffi-

ciently high concentration gradient of surfactant ions accumulated within a particle surface layer will generate an electric field. According to Semenov, this phenomenon, termed as concentration polarization, could cause apparent changes in the thermophoretic mobility of a particle, as well as a macroscopic effective concentration gradient of surfactant and an electric field in a suspending liquid.

The most recent work by Schimpf and Semenov [17] focuses on the effect of salt in the suspending medium on thermophoresis and reported that thermophoretic behavior of dissolved polymers, solid particles and latex emulsions cannot be described by a common physicochemical mechanism. For instance, the previously observed increases in thermophoretic mobilities of latex particles upon addition of salt to the suspending medium cannot be related solely to electrostatic effects as is the case with solid particles such as silica (and by extension, metal particles). The authors proposed that the thermophoresis of latex particles (considered as droplets of polymer solution in a polar solvent emulsion) is due to that of the polymer chains partitioning between the solvent inside the droplet and the surrounding polar solvent. The model postulates that the thermophoretic mobility of latex particles increases from zero to a hypothetical value for polymer in the polar solvent as the square of the derived dimensionless parameter (which represents the product of the monomer concentration at the particle surface, the monomer radius and the square of the mean thickness of the monomer unit distribution in the external solvent) increases. The model yields thermophoretic mobilities of polystyrene latex particles in water and acetonitrile comparable to that in nonpolar solvents.

In this present study, ThFFF retention data for various submicrometer metal particles suspended in both aqueous and nonaqueous carrier liquids were determined, and the results compared with those obtained for nonmetallic particles such as silica and latex particles. The relative thermophoretic velocities of these particles are inferred from the magnitude of their retention in a thermal field-flow fractionation channel and the corresponding retention expression for ThFFF. Influence of field strength (measured as temperature drop, ΔT across the ThFFF walls) on the retention of metal particles was also investigated and

the results used to illustrate the dependence of thermophoretic velocity of metal particles on ΔT. In addition, the effect of the presence of an electrolyte in either aqueous or nonaqueous carrier liquids was investigated and the results compared with earlier observations with latex and/or silica particles [1,2,12,13].

In the accompanying sections, a brief description of field-flow fractionation techniques and the relevant theoretical models for ThFFF are provided. The latter is significant since it is the technique used to illustrate thermophoresis of metal particles suspended in both aqueous and nonaqueous media.

1.1. Field-flow fractionation

Field-flow fractionation (FFF) is a family of separation techniques whose operation is based on subjecting a sample to the combined effects of an external field applied perpendicular to the axis of a thin, open fractionation channel and to the axial flow of carrier liquid through the channel. Separation of the sample components occurs due to the differential interaction of the external field with the various sample components, which displaces them unequally towards the channel accumulation wall. Following the unequal displacement, different sample components end up in different stream laminae with unequal velocities. The final result is differential component elution [21]. Each external field (or gradient) yields a unique FFF technique, with the most commonly used FFF "fields" being thermal gradients, cross-flow driving forces and sedimentation fields. These "fields" yield the techniques of thermal FFF (ThFFF), flow FFF, and sedimentation FFF, respectively.

In ThFFF, the external "field" is a temperature gradient applied across a channel enclosed between two parallel, highly polished metal bars. The temperature gradient induces displacement of macromolecular and particulate sample materials by thermal diffusion [22] in a carrier liquid toward one wall (the accumulation wall) of the channel leading to separation.

ThFFF has traditionally been used for the separation and characterization of polymers of molecular masses ranging from 10^4 to 10^7 and up [22–25] because of its intrinsically high selectivity. The

applications of ThFFF have however, been expanded to include separation of particulate materials of varied chemical composition over the submicrometer and larger size range suspended in either aqueous or nonaqueous carrier solutions [1,2,11–13]. Evaluation of thermal diffusion coefficient data of a number of latexes and silica particles suspended in either aqueous or nonaqueous carrier systems have been made possible with the help of the ThFFF technique [1,2].

2. Theory

The standard model for retention of sample components in normal mode FFF is expressed as [26,27]:

$$t_R/t^0 = 1/6\lambda[\coth(1/2\lambda) - 2\lambda] \qquad (1)$$

where t_R is the retention time of a sample component, t^0 is the channel void time (time needed to elute a nonretained component of the sample) and λ is a dimensionless retention parameter (defined as $\lambda = l/w$, where l is the mean thickness of the sample component zone compressed against the accumulation wall, i.e. the distance from the cold wall to the center of gravity of the component zone, and w is the channel thickness). The dimensionless parameter λ is a measure of the extent of interaction between the externally applied field or gradient and the sample component.

Eq. (1) is however, an oversimplification for ThFFF and for rigorous studies it must be corrected to account for distortions to the parabolic flow profile arising from viscosity changes caused by the temperature gradient applied across the channel [28,29]. However, despite the oversimplification with respect to ThFFF, Eq. (1) still yields a reasonably accurate mathematical form even with further approximations. For example, the limiting form of Eq. (1) for highly retained sample components (i.e. $\lambda \rightarrow 0$) is:

$$t_R/t^0 = 1/6\lambda \qquad (2)$$

Since λ is a measure of the level of interaction between sample components and the applied field or gradient, it can be expressed as [30,31]:

$$\lambda = D/D_T\Delta T \qquad (3)$$

where D is ordinary concentration diffusion coefficient of sample component, D_T is its thermal diffusion coefficient, and ΔT is the temperature drop across the hot and cold walls of the ThFFF channel.

Combining Eqs. (2) and (3), we obtain:

$$t_R/t^0 = 1/6\lambda = D_T\Delta T/6D \qquad (4)$$

From Eq. (4) it is clear that retention in ThFFF is controlled by two transport processes: ordinary concentration diffusion and thermal diffusion [22] and that at constant ΔT, differences in sample component retention time suspended in the same carrier liquid is attributable to differences in the two transport processes. Whereas D is related to particle size, d, temperature, T, and solution intrinsic viscosity, η by the Stokes–Einstein expression (i.e. $D = kT/3\pi\eta d$), the parameters that influence D_T are not yet well understood. Substitution of the Stokes–Einstein expression for D into Eq. (4) yields:

$$t_R/t^0 = \pi\eta dD_T\Delta T/2\,kT \qquad (5)$$

It is apparent from Eq. (5) that sample particles of equal size suspended in the same carrier solution and subjected to the same ΔT will have different retention times because of different D_T values.

According to studies by various workers [1,2,10,12,13,18–20], several factors have been identified empirically as influencing particle retention and therefore by extension influencing D_T in ThFFF. These factors include size and chemical composition of particle and carrier liquid. Theories developed by Semenov [15,16] attempt to provide a qualitative basis for the understanding of some of these observations and also appear useful in explaining our present observations of thermophoresis of metal particles as studied by ThFFF.

3. Experimental

The ThFFF system used for this work is similar in design to the model T100 polymer fractionator from FFFractionation (now PostNova Analytics, Salt Lake City, UT, USA). Most components of the system, including the ThFFF channel, have previously been used for other aqueous and nonaqueous particle studies [12,13]. The channel volume was cut from a 76-μm (127 μm was used in some cases) thick

Mylar spacer and was rectangular in shape with tapered ends. The breadth measured 2.0 cm and the distance between the inlet and the outlet was 44.6 cm.

The channel spacer was confined between two chrome-plated copper bars, with the top bar heated using rods controlled by relay switches with on and off cycle times activated by a microprocessor and controlled by user input. The cold wall was cooled using continuously flowing tap water. Temperatures in the cold and hot walls were monitored by inserting two thermal sensors into wells which were drilled into both top and bottom bars.

Aqueous solution and Spectrograde tetrahydro-furan (THF) and acetonitrile (ACN) were used as carrier liquids in this study. These solutions were delivered using a Model M-6000A pump from Waters (Milford, MA, USA). The Spectrograde THF and ACN were obtained from EM Science (Cherry Hill, NJ, USA). The aqueous carriers consisted of doubly distilled deionised water containing 0.02% sodium azide plus 0.10% Aerosol-OT (Fisher Scientific, Fair Lawn, NJ, USA) as a surfactant. The ionic strength of the organic carriers was adjusted using 0.10 mM tetrabutyl ammonium perchlorate (TBAP). The flow-rate used was 0.30 ml/min (unless stated otherwise) and the sample injection volume was 20 µl. A pressure regulator was attached to hold the channel outlet pressure at 100 p.s.i. above atmospheric pressure. Unless otherwise stated, the cold wall temperature was between 294 and 297 K.

A model UV-106 detector from Cole Scientific (Calasabas, CA, USA) operating at 254 nm wavelength was used to detect particles eluting from the ThFFF channel. Data acquisition of the detector signal was made possible using a PC-AT compatible computer. The detector signal was recorded using an OmniScribe chart recorder from Houston Instruments (Austin, TX, USA).

The sample particles used in this study were comprised of metals and nonmetals. The 0.250 µm silica from Merck (Darmstadt, Germany) and 0.197 and 0.304 µm polystyrene (PS) particles from Dow (Midland, MI, USA) made up the nonmetals. The metal particles were 0.2 ± 0.10 µm palladium (Pd), 0.3 ± 0.10 µm silver (Ag), 0.3 ± 0.10 µm gold (Au), and 0.3 ± 0.10 µm platinum (Pt). We confirmed that Pd was the smallest size using scanning electron

microscopy. All the metal particles were obtained from Degussa (South Plainfield, NJ, USA). Stop flow relaxation was used in all the experiments unless otherwise stated.

4. Results and discussion

4.1. Effect of carrier composition

Fig. 1 shows superimposed ThFFF elution profiles of submicrometer metal and silica particles suspended in an aqueous carrier solution made up of 0.1% Aerosol-OT as a surfactant plus 3.0 mM of sodium azide (NaN$_3$). The NaN$_3$ is a common additive in particle separations by FFF and acts as both a bacteriocide and an electrolyte. The Aerosol-OT was used because it provided the most stable metal particle suspensions. The ΔT used with the metal and silica particles were 78 and 40 K, respectively. Three interesting observations can be made
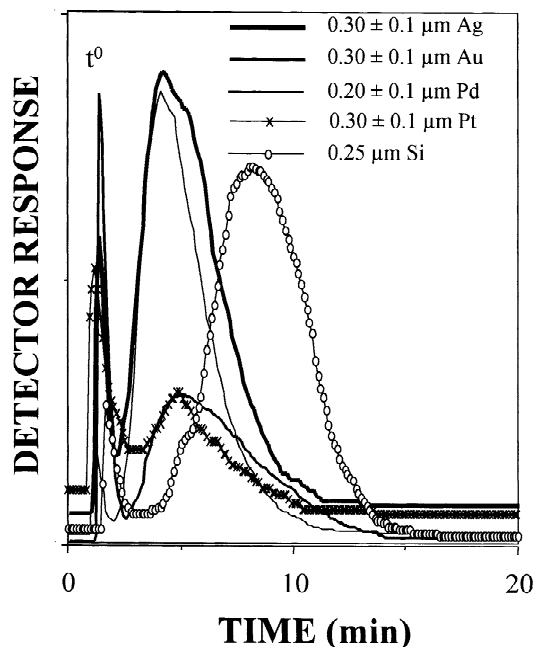

Fig. 1. Elution profiles for metal and silica particles suspended in an aqueous solution composed of 0.1% Aerosol-OT and 3.0 mM sodium azide. Experimental conditions: flow-rate 0.32 ml/min, $\Delta T=40$ K for silica and 78 K for the metal particles and $w=76$ µm.

from this figure. First, it is clear that despite the large difference in the field strengths employed between the two particle types (i.e. silica versus metal), silica is still retained the most. Second, the relatively smaller size silica particles (except for the 0.2 ± 0.10 μm Pd) is retained longer than the relatively larger size (0.3 ± 0.10 μm) metal particles. Finally, despite the compositional variations among the metal particles, their elution profiles overlap (alongside the smaller Pd).

Following the above observations, some general conclusions can be made. That despite the assumption that the metal particles cannot maintain large temperature gradients across their surfaces due to their high thermal conductivities [5], higher than expected thermophoresis of metal particles is still possible in an aqueous medium. This observation is consistent with the previously proposed model for thermophoresis of solid particles, which predicts higher than expected thermophoretic mobilities for metal particles [10]. The model is based on the osmotic pressure gradient produced by the temperature dependence on the concentration of accumulated charges on the solid particle surface. The presence of NaN_3 in solution is the origin of the expected accumulated charges on the metal particle surface. Hence the basis for the increased temperature gradient across the metal particle surface. The longer retention of the silica particles (even with the lower ΔT) however, still suggests higher thermophoretic mobility for the silica than the metal particles in an aqueous suspension. This could be attributed to a greater ability of the electrolyte ions to adsorb on the silica than on the metal particles, thereby establishing a more significant double layer at the silica surface. Hence a greater osmotic pressure gradient. The possible association of the Aerosol-OT surfactant with the silica surface cannot be ruled out also to achieve a similar (or greater) effect on the osmotic pressure gradient. The co-elution of the smaller size (0.2 ± 0.10 μm) Pd and the rest of the larger size (0.3 ± 0.10 μm) metal particles is also consistent with the osmotic pressure gradient model [10] which does not predict any particle thermophoretic mobility dependence on size. However, the difference in retention behavior between the silica particles and metal particles is consistent with previous observa-
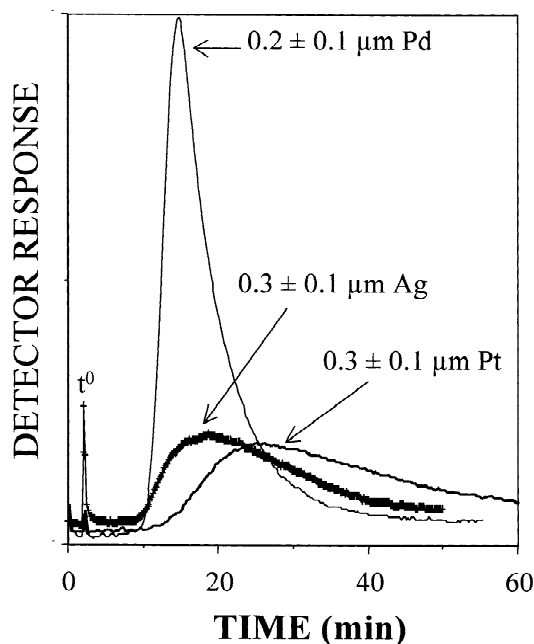

Fig. 2. Elution profiles of particles suspended in ACN plus 0.10 mM TBAP carrier solution. Experimental conditions: flow-rate 0.32 ml/min, $\Delta T = 38$ K and $w = 76$ μm.

tions on the retention dependence on chemical composition [1,2,12,13,18–20].

The situation, however, changes when a nonaqueous carrier solution is employed. Fig. 2 shows superimposed elution profiles of the Ag, Pd, and Pt particles obtained with a reduced field strength of $\Delta T = 38$ K in a 0.10 mM TBAP-containing ACN carrier solution. The electrolyte concentration used here is an order of magnitude less than what was used with the aqueous carrier of Fig. 1. It is evident from Fig. 2 that the elution profiles of the metal particles no longer overlap as was the case in Fig. 1. The peak maxima for the Pd, Ag and Pt particles appear at about 15.0, 18 and 24.2 min, respectively. These measured retention times in ACN are nearly three times longer than the values recorded for the same metal particles with the aqueous carrier solution of Fig. 1 (despite the lower ΔT value of 38 K with ACN than the ΔT of 78 K with the aqueous medium). This implies that the metal particles have much higher thermophoretic mobilities in ACN than

in the aqueous carrier solution. Aside from the expected differences in the extent of formation of concentration polarization between the two solvent types (due to polarity differences), we do not have any other plausible explanation for this difference in thermophoretic behavior. However, these results reflect the strong dependence of metal particle retention on the composition of the suspending media as has been previously observed with latex and silica particles [2–4,12,19,20].

Solvent-compositional effects on thermophoretic mobility are evident even among different nonaqueous carrier solutions (rather than between aqueous and nonaqueous). Fig. 3 shows superimposed elution profiles of Pd metal particles suspended in THF and ACN. Both carrier solutions contained 0.10 mM TBAP. It is evident from the figure that the retention of Pd metal particles is lower in THF than in ACN. This could be explained in terms of the different ability of TBAP to associate with the metal surfaces
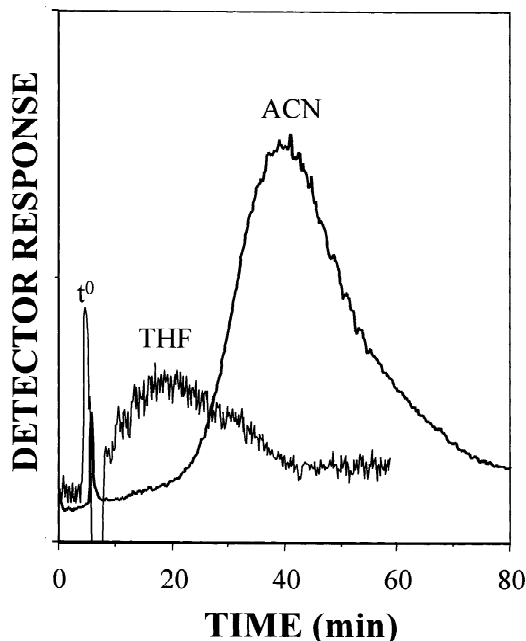
Fig. 3. Elution profiles for 0.2±0.10 μm Pd particles suspended in ACN and THF carrier solutions. Experimental conditions: flow-rate 0.32 ml/min, [TBAP]=0.10 mM, ΔT=30 K and w=127 μm.

in the two carrier systems. Similar trends were observed with the other metal particles and the results are omitted here for reasons of brevity. This implies that thermophoretic mobility of metal particles is influenced by the chemical composition of the suspending medium (between and among aqueous and nonaqueous carriers).

4.2. Effect of ionic strength

From the literature, it is apparent that the retention of latex and silica particles is significantly influenced by the ionic strength of the carrier suspension employed [1,2,11–13,19,20]. It was therefore necessary to examine the validity of this generalized view in the case of metal particles. Experiments were carried out in both aqueous and acetonitrile carrier solutions. Fig. 4a shows the near lack of retention of all the metal particles studied using an electrolyte- (or surfactant-) free aqueous carrier. The carrier liquid was doubly distilled deionised water with the rest of the experimental conditions identical to those of Fig. 1. The results of Fig. 4a contrasts sharply with those of Fig. 1 and shows that the retention of metal particles in ThFFF is affected by the presence of an electrolyte in an aqueous carrier solution. Similar results were observed when nonaqueous carrier solutions of ACN and THF were used. Fig. 4b shows two superimposed elution profiles for Pd metal particles: one with and the other without an electrolyte. The rest of the experimental conditions are similar to those for Fig. 2. Here too, the retention of Pd particles is reduced in the absence of the electrolyte. The elution profile for Pd in the presence of 0.10 mM TBAP in this figure matches that of Fig. 2 (peak maximum at about 18 min). It can therefore be concluded that, just like with latex and silica particles, the retention of metal particles is also influenced by the ionic strength of the carrier media (aqueous and nonaqueous) and that for effective retention of metal particles in a ThFFF channel, electrolyte-containing carriers should be employed. However, it is significant to note that despite the apparent dependence of metal particle retention on electrolyte concentration (in both aqueous and nonaqueous carrier systems), appreciable retention of the metal particles is still possible in an electrolyte-
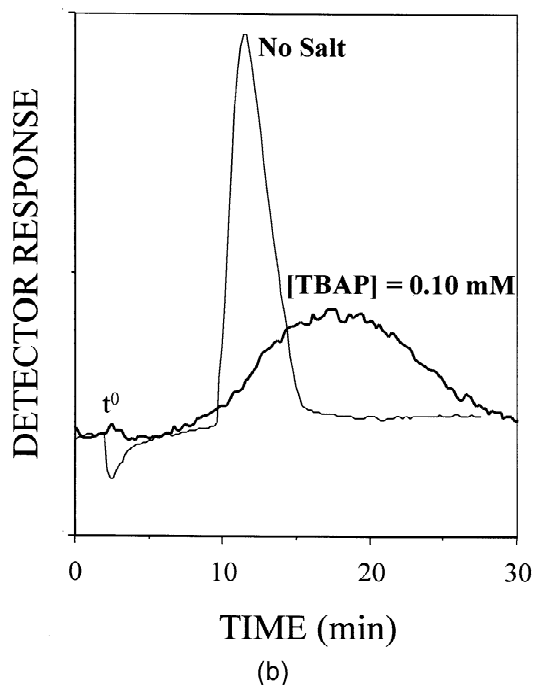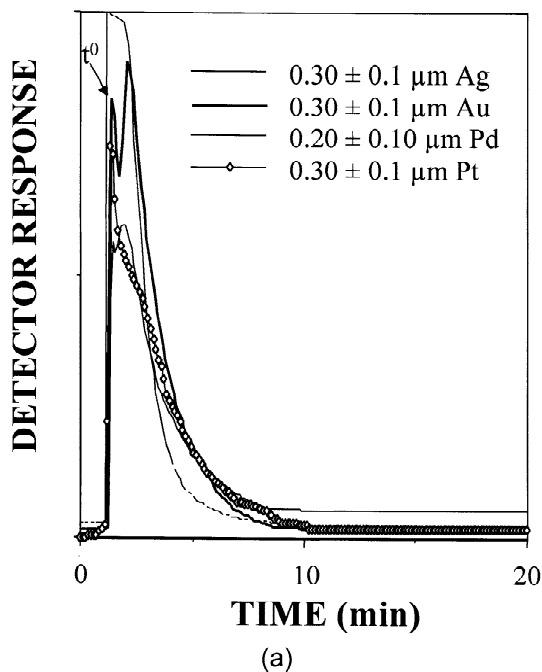
Fig. 4. (a) Elution profiles of Ag, Au, Pd and Pt particles suspended in doubly distilled deionised water. Experimental conditions: flow-rate 0.32 ml/min, $\Delta T = 78$ K and $w = 76$ μm. (b) Elution profiles for Pd particles obtained in the absence and presence of 0.10 mM TBAP in ACN as carrier. Experimental conditions: flow-rate 0.32 ml/min, $\Delta T = 38$ K, and $w = 76$ μm.

free nonaqueous carrier such as ACN. Fig. 4b shows complete separation of the Pd peak from the void peak in an electrolyte-free ACN carrier, unlike the results shown in Fig. 4a obtained with an aqueous carrier. This observation was also evident with electrolyte-free THF, although the level of retention in THF is lower than in ACN.

Additional results showing appreciable retention of the other metal particles (as well as 0.304-μm PS beads) in an electrolyte-free ACN are given in Fig. 5. This figure also provides interesting revelations. First, in contrast to the results of Fig. 1 which showed overlapped elution profiles for the metal particles (despite the difference in size between Pd and the other metal particles), the electrolyte-free ACN provided different retention magnitudes for the metal particles. The smaller 0.2 ± 0.10 μm Pd particles are retained less than the 0.3 ± 0.10 μm Pt and Ag particles. Second, it is also interesting to note that the 0.304-μm PS latex particles are retained to a lesser extent than the equal sized Ag and Pt metal particles.
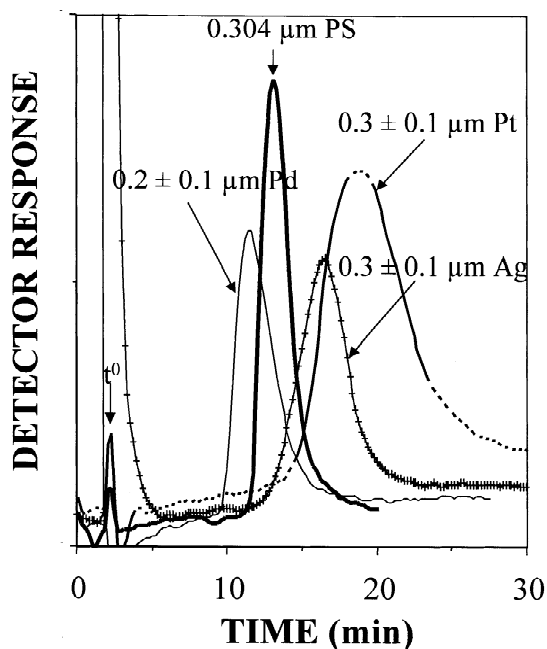
In earlier studies involving the retention of latex

Fig. 5. Elution profiles for Ag, Pd and Pt and 0.304 μm PS particles in electrolyte-free ACN. Experimental conditions: flow-rate 0.30 ml/min, $\Delta T = 38$ K, and $w = 76$ μm.

and silica particles in ThFFF [1,2], particle–wall electrostatic interactions of a repulsive nature was proposed as the mechanism behind the reduced retention times in electrolyte-free aqueous and nonaqueous carriers. However, recent studies by Jeon and co-workers [3,19,20] suggest that effects from electrostatic phenomena are not great enough to fully explain the dependence of retention on ionic strength in aqueous media. They attribute the latex or silica particle retention dependence on ionic strength to changes in the surface tension of the particles. They however, conclude that surface tension phenomenon may not be applicable to solid particles (except for silica) such as the metal particles reported in this present paper.

The recent model proposed by Semenov [16] which considers thermophoresis of solid particles as a surface-driven phenomena, is the best suited to explain the observed thermophoretic behavior of metal particles in electrolyte-containing aqueous and nonaqueous carriers. According to Semenov, the phoretic movement of particles arises from the osmotic pressure gradient and/or the electrostatic force in the particle surface layer where surfactant molecules or electrolyte ions are accumulated. With this model, an electrostatic force acts on the noncompensated diffuse electric charge (which exists in the double electric layers) when the particle is suspended in an electrolyte. As a result of the osmotic pressure gradient (probably caused by both macroscopic temperature and surfactant concentration gradient), "slipping" of the liquid in the surface layer arises, which leads to either particle phoresis or to the osmotic flow of the liquid when the solid particle surface does not yield. This could be used to account for the increase in retention time of the metal particles suspended in the surfactant- (and/or electrolyte-) containing aqueous medium shown in Fig. 1. However, what is not yet clear, is the origin of thermophoresis in electrolyte-free nonaqueous carrier suspensions. Sample overloading effects (since ionic strength and amount of sample injected would influence interparticle interactions) were ruled out as a possible cause for the observed ionic strength effects by carrying out overloading studies. The results of the overloading studies are omitted.

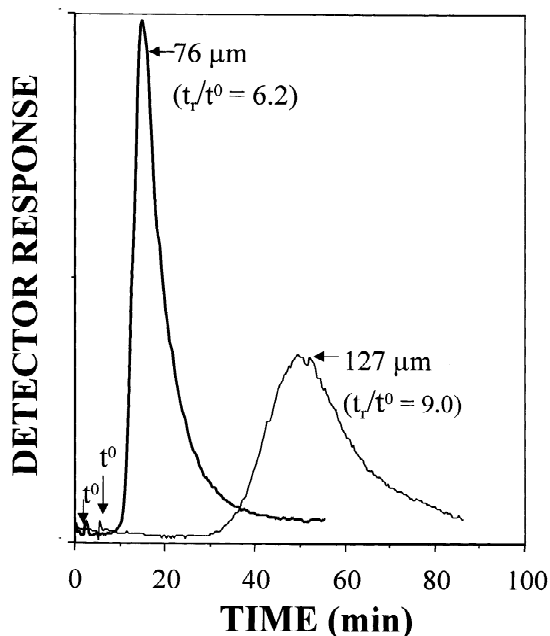The effect of channel thickness on the retention of the metal particles was also investigated. Fig. 6

Fig. 6. Elution profiles for Pd particles suspended in ACN containing 0.10 mM TBAP obtained using $w = 76$ μm and $w = 127$ μm. The carrier flow-rate, 0.30 ml/min and $\Delta T = 38$ K.

shows two superimposed elution profiles of Pd particles suspended in ACN obtained with two channels of different thicknesses (i.e. 76 and 127 μm) under a constant ΔT of 38 K. A uniform volumetric flow-rate of 0.30 ml/min was maintained in both cases, thereby guaranteeing a shorter sample residence time with the thinner channel spacer. As shown in the figure, the thicker channel yielded a larger t_R/t^0 ratio of 9.0 compared to a value of 6.2 for the thinner channel spacer. This was surprising since the thinner channel spacer yields a higher temperature gradient (dT/dx) of $5.0 \cdot 10^3$ K cm^{-1} compared to $3.0 \cdot 10^3$ K cm^{-1} for the thicker channel. (The temperature gradient is assumed to be linear across the channel spacer and that $(dT/dx) \cdot w \approx \Delta T$, where T is absolute temperature, x is the distance measured from the accumulation wall and w is the channel thickness.) Unfortunately, we do not have any explanation for this observation and recommend that further investigations be conducted. However, based on this result, we recommend the use of larger channel thickness for improved metal particle retention in ThFFF.

4.3. Effect of gravitational field

In order to ascertain that the observed retention profiles of the metal particles was primarily due to the applied ΔT and not the earth's gravitational force, retention profiles of the metal particles were obtained both in the presence and absence of ΔT. Fig. 7a shows superimposed elution profiles of Pt metal particles obtained in an electrolyte-containing ACN at two separate conditions corresponding to ΔT of 0 and 40 K (both with $w = 76$ μm). It is apparent from this figure that the Pt particles elute with insignificant separation from the void peak when $\Delta T = 0$ K. However, a $\Delta T = 40$ K afforded a significant retention of the Pt particles. Similar results were obtained with the other metal particles and are omitted here for reasons of brevity. This implies that the contribution of the gravitational force to the observed Pt particle retention is negligible. The contribution of the gravitational field on the retention of Pd particles was also investigated using a channel thickness of 127 μm and the results are shown in Fig. 7b. Here too, the contribution of the gravitational force was negligible under the flow conditions employed.

4.4. Effect of ΔT

The effect of ΔT on the retention of the metal particles was examined in both electrolyte-free and electrolyte-containing ACN carrier medium. The reduced retention time (t_R/t^0) data were obtained under two different ΔT conditions of 40 and 60 K. The results are summarized in Table 1. An increase in ΔT causes an increase in the retention time of all the metal particles studied (even in the absence of an electrolyte). Similar experiments in an aqueous carrier were however not carried out due to the relatively low thermophoretic mobilities observed for the metal particles even at a high ΔT of 78 K in electrolyte-containing aqueous media (see Fig. 1).

Additional results showing the influence of ΔT on the retention of Pd metal particles in an electrolyte-containing ACN are given in Fig. 8a. The electrolyte-containing ACN not only offers longer retention times for Pd particles but also larger increases in retention times with increases in ΔT. A ΔT value as low as 10 K is sufficient to produce a
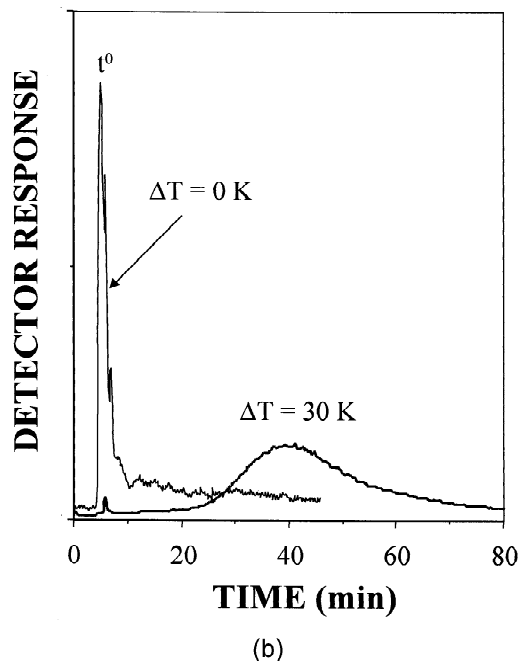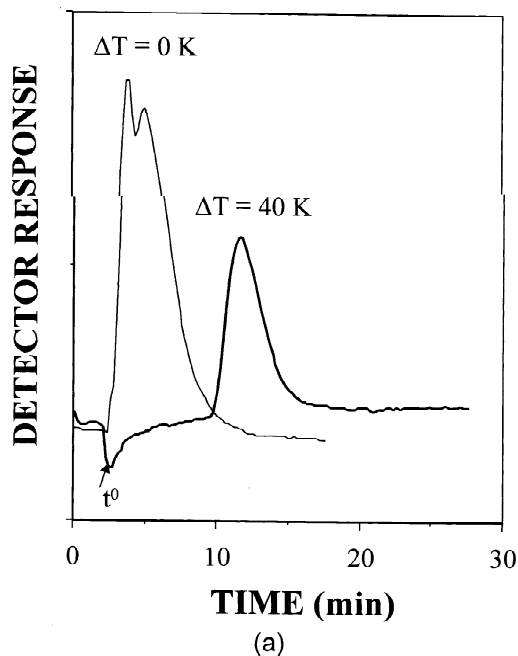

(a)

(b)

Fig. 7. (a) Elution profiles for Pd particles in ACN plus 0.10 m*M* TBAP obtained at two different ΔT values of 0 K (simulating only gravitational field force) and 40 K. The carrier flow-rate was 0.30 ml/min and $w = 76$ μm. (b) Elution profiles of Pd particles in ACN plus 0.10 m*M* TBAP obtained at two different ΔT values of 0 K (simulating only gravitational field force) and 30 K. The carrier flow-rate was 0.30 ml/min and $w = 127$ μm.

Table 1
Effect of ΔT on the reduced retention time (t_R/t^0) of metal particles in an electrolyte-free ACN carrier liquid; the carrier flow-rate was 0.30 ml/min and $w = 76$ μm

Sample	t_R/t^0 at $\Delta T = 40$ K	t_R/t^0 at $\Delta T = 60$ K
Ag	5.66	7.63
Au	5.89	7.85
Pd	5.59	7.35
Pt	6.97	8.25

near-complete separation of the Pd particles from the void peak: a retention much larger than that obtained with a $\Delta T = 60$ K in an electrolyte-free ACN. A corresponding plot of reduced retention time (t_R/t^0) versus ΔT is linear as shown in Fig. 8b. This is in agreement with the theoretical expression shown by Eq. (5).

4.5. Effect of carrier flow-rate

To further improve elution speed while maintaining reasonable sample retention, the effect of higher carrier flow-rates on particle elution profiles and speed were investigated. The carrier liquid used was ACN containing 0.10 mM concentration of TBAP and the ΔT was 40 K. Fig. 9 shows superimposed elution profiles of Pd particles obtained under different flow-rates of 0.30, 0.50 and 0.70 ml/min. The figure shows a general increase in retention time of the Pd particles with decrease in flow-rate as exemplified by the calculated ratios of t_R/t^0 of 7.3, 8.0 and 9.0 for 0.70, 0.50 and 0.30 ml/min, respectively. These flow-rate experiments were done without using stop-flow relaxation. The observed trend of lowest t_R/t^0 for highest flow-rate is as expected. However, the magnitude of the changes may not represent the true extent of the particle retention in the ThFFF channel due to insufficient sample relaxation. Nevertheless, these experiments show that higher flow-rate regimes can still be employed with metal particles without compromising their complete separation from the void peak in a ThFFF system.

4.6. Effect of sample composition

The influence of composition on the retention of latex and silica particles in both aqueous and nonaqueous carrier media by ThFFF has previously
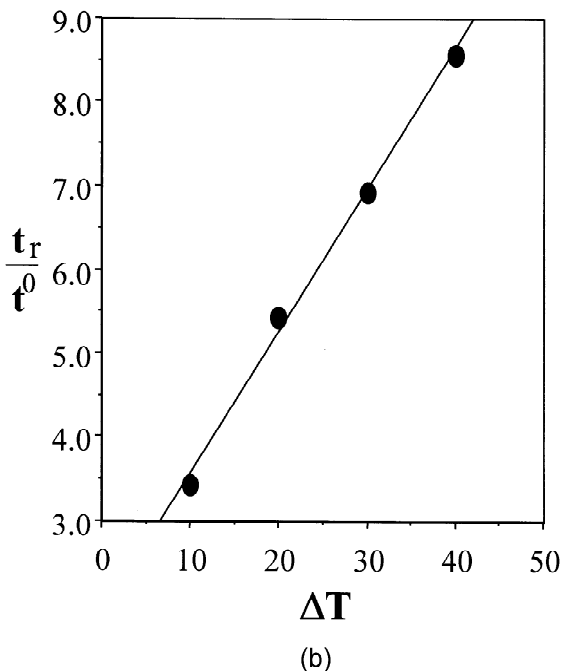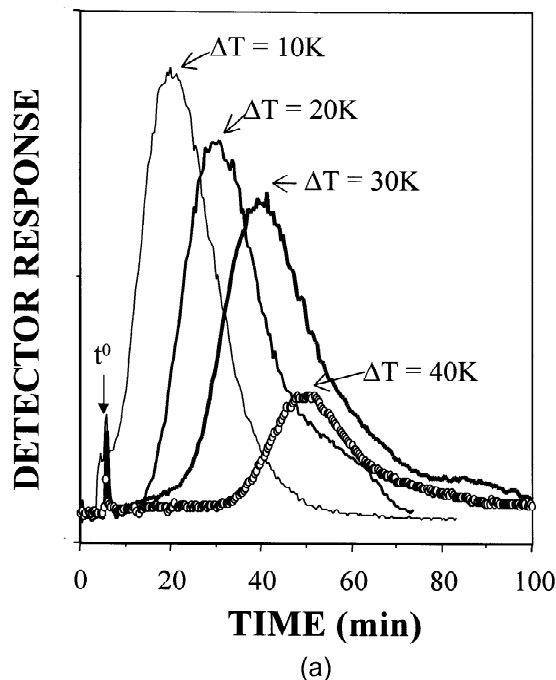

(a)

(b)

Fig. 8. (a) Effect of ΔT on the retention of Pd particles suspended in TBAP-containing ACN carrier liquid. The carrier flow-rate was 0.30 ml/min and $w = 127$ μm. (b) Plot of reduced retention time (t_R/t^0) versus ΔT for Pd particles suspended in TBAP-containing ACN carrier liquid. The flow-rate was 0.30 ml/min and $w = 127$ μm.

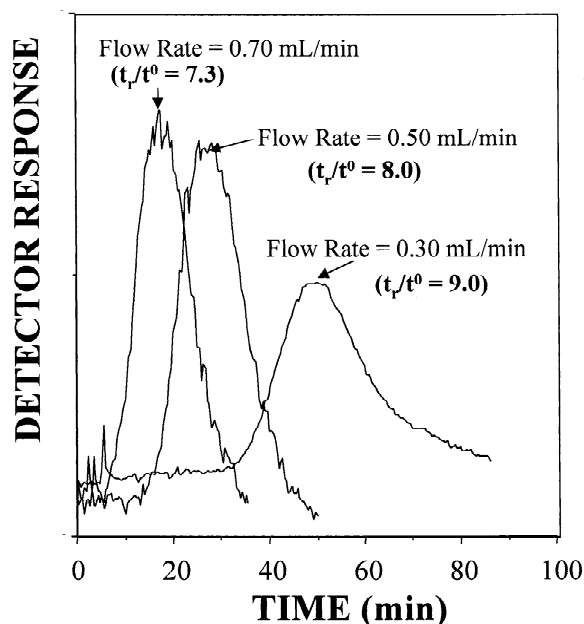Fig. 9. Effect of flow-rate on the retention of Pd particles in ACN plus 0.10 mM TBAP carrier liquid; $\Delta T = 40$ K and $w = 127$ μm.

Fig. 10. Superimposed elution profiles of 0198 μm PS, 0.2±0.10 μm Pd, and 0.3±0.10 μm Pt particles in ACN carrier containing 0.10 mM TBAP. Carrier flow-rate was 0.70 ml/min, $\Delta T = 40$ K and $w = 127$ μm.

been demonstrated and reported elsewhere [2,3,12,18,19]. In this paper we provide additional results of compositional effects on the retention of metal particles by ThFFF. Fig. 10 shows superimposed elution profiles of 0.198 μm PS, 0.2±0.10 μm Pd and 0.3±0.10 μm Pt particles suspended in ACN containing 0.10 mM concentration of TBAP. The relatively smaller size PS particles are retained longer than either the larger (Pt particles) or comparable (Pd particles) sized metal particles. These results contrast sharply with those obtained for the electrolyte-free ACN of Fig. 5, in which the larger 0.304-μm PS particles had comparable retention with the smaller sized Pd particles. Note that from Fig. 5, the retention of the 0.304-μm PS is still lower than that for either Pt or Ag particles, whereas the retention of 0.198-μm PS is now much larger in an electrolyte-containing ACN (see Fig. 10). The larger retention of the 0.198-μm PS in electrolyte-containing ACN gives further credence to the model proposed by Semenov and Schimpf [17], which focuses on the role of salt in the suspension medium. In our experiments, the presence of TBAP should increase the solubility of the PS monomer units
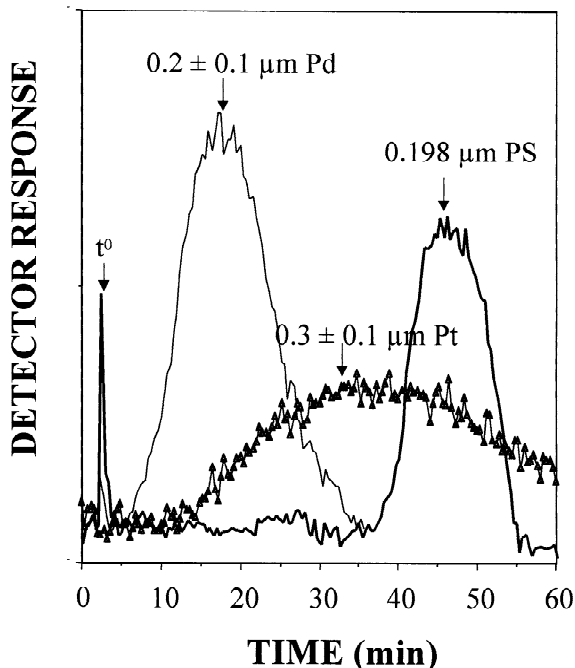
within the barrier film (i.e. film of surfactant that surrounds the particle and serves as a barrier to monomers during the emulsion polymerization process) around the latex particle and beyond into the external solution. The "external" monomer units are expected to undergo strong thermophoresis and thus dominate the movement of the latex particles in a temperature gradient. Hence the greater thermophoretic mobilities of the 0.198-μm PS latex compared to the relatively larger-size Pd and Pt particles in TBAP-containing solution.

5. Conclusion

This study shows that ThFFF is capable of retaining metal particles suspended in either aqueous or nonaqueous carrier solutions. Like latex and inorganic silica particles, the retention of metal particles is influenced by several factors including chemical

composition, salt concentration, carrier solution composition and field strength.

The retention of metal particles increases with the addition of salt to either an aqueous or organic carrier solution. The 3.0 mM concentration of NaN$_3$ in a 0.1% Aerosol-OT-containing aqueous medium did not however, yield as significant an increase in retention as did the addition of 0.10 mM TBAP in ACN carrier solution. It is interesting to note that, metal particles are significantly retained in a salt-free ACN carrier in comparison to the near-lack of retention in a salt-free aqueous carrier (even with twice as high a value in ΔT). It is clear that the thermophoretic mobilities of the metal particles are greater in ACN than in aqueous carrier solution. This observed effect of salt on retention supports the proposal that the mechanism of thermophoresis of solid particles is based on the osmotic pressure gradient produced by the temperature dependence in the concentration of accumulated charges on the particle surface [10]. The observed thermophoretic mobilities of the metal particles in a salt-free ACN carrier is however, still puzzling and needs to be further investigated. This study also reveals that the level of retention of metal particles is dependent on the composition of the suspending medium (between and/or among aqueous and nonaqueous). Among nonaqueous carrier solutions for instance, palladium metal particles are more retained in ACN than in THF (both containing 0.10 mM TBAP). In addition, metal particle retention is also dependent on their chemical composition, which is more evident in ACN carrier solution. It is also apparent that the relationship between composition and retention is significantly affected by the presence of salt. It is evident that presence of salt in ACN affords longer retention for PS latex particles (of even a smaller diameter) than metal particles, unlike in the absence of salt where metal particles of comparable sizes are retained longer than PS particles of comparable size.

6. Nomenclature

d particle diameter
D ordinary diffusion coefficient
D_T thermal diffusion coefficient
k Boltzmann's constant
l mean layer thickness of sample cloud
R retention ratio
t_R retention time
t^0 channel void time
T temperature
T_c cold wall temperature
w channel thickness
ΔT temperature drop applied across channel
η viscosity
λ retention parameter

Acknowledgements

References

[1] G. Liu, J.C. Giddings, Chromatographia 34 (1992) 483.
[2] P.M. Shiundu, G. Liu, J.C. Giddings, Anal. Chem. 67 (1995) 2705.
[3] S.J. Jeon, M.E. Schimpf, A. Nyborg, Anal. Chem. 69 (1997) 3442.
[4] E.P.C. Mes, R. Tijssen, W.Th. Kok, J. Chromatogr. A 907 (2001) 201.
[5] B.V. Derjaguin, S.S. Dukhin, A.A. Korotkova, Kolloidn. Zh. 23 (1961) 53.
[6] E. Ruckenstein, J. Colloid Interface Sci. 83 (1981) 77.
[7] M.M. Williams, J. Colloid Interface Sci. 22 (1988) 110.
[8] J.L. Anderson, Annu. Rev. Fluid Mech. 21 (1989) 61.
[9] G.S. McNab, A. Meisen, J. Colloid Interface Sci. 44 (1973) 339.
[10] J.C. Giddings, P.M. Shiundu, S.N. Semenov, J. Colloid Interface Sci. 176 (1995) 454.
[11] G. Liu, J.C. Giddings, Anal. Chem. 63 (1991) 328.
[12] P.M. Shiundu, J.C. Giddings, J. Chromatogr. A 715 (1995) 117.
[13] P.M. Shiundu, E.E. Remsen, J.C. Giddings, J. Appl. Polym. Sci. 60 (1996) 1695.
[14] M.E. Schimpf, S.N. Semenov, J. Phys. Chem. B 104 (2000) 9935.
[15] S.N. Semenov, J. Liq. Chromatogr. Rel. Technol. 20 (1997) 2687.
[16] S.N. Semenov, J. Microcol. Sep. 9 (4) (1997) 287.
[17] M.E. Schimpf, S.N. Semenov, J. Phys. Chem. B 105 (2001) 2285.

[18] S.K. Ratanathanawongs, P.M. Shiundu, J.C. Giddings, Colloids Surf. A 105 (1995) 243.

[19] S.J. Jeon, M.E. Schimpf, Polym. Mater. Sci. Eng. 75 (1996) 4.

[20] S.J. Jeon, M.E. Schimpf, Thermal field-flow fractionation of colloidal particles, in: T. Provder (Ed.), Particle Size Distribution III: Assessment and Characterization, American Chemical Society Symposium Series No. 693, Washington, DC, 1998, p. 182, Chapter 13.

[21] J.C. Giddings, Science 260 (1993) 1456.

[22] J.J. Gunderson, J.C. Giddings, Macromolecules 19 (1986) 2618.

[23] H. Thompson, M.N. Myers, J.C. Giddings, J. Sep. Sci. 2 (1967) 797.

[24] J.C. Giddings, M. Martin, M.N. Myers, J. Chromatogr. 158 (1978) 419.

[25] J.C. Giddings, V. Kumar, P.S. Williams, M.N. Myers, Polymer separation by thermal field-flow fractionation: high speed power programming, in: C.D. Craver, T. Provder (Eds.), ACS Advances in Chemistry Series Polymer Characterization: Physical Property, Spectroscopic, and Chromatographic Methods, Vol. 227, ACS, Washington, DC, 1990, Chapter 1.

[26] J.C. Giddings, Sep. Sci. Technol. 19 (1984) 831.

[27] J.C. Giddings, Chem. Eng. News 66 (1988) 34.

[28] A.C. van Asten, H.F.M. Boelens, W.Th. Kok, H. Poppe, P.S. Williams, J.C. Giddings, Sep. Sci. Technol. 29 (1994) 513.

[29] J.J. Gunderson, K.D. Caldwell, J.C. Giddings, Sep. Sci. Technol. 19 (1984) 667.

[30] M.N. Myers, K.D. Caldwell, J.C. Giddings, Sep. Sci. 9 (1974) 47.

[31] R. Sisson, J.C. Giddings, Anal. Chem. 66 (1994) 4043.